Research on Engineering Structures & Materials
journal homepage: http://www.jresm.org
MIM Research Group

Research Article

Parametric optimization of ball milling process parameters for uniform distribution of particles

Rashmi Arya*,[a], Hari Singh[b]

Department of Mechanical Engineering, National Institute of Technology, Kurukshetra

Article Info

Article history:

Received 14 June 2023
Accepted 04 Sep 2023

Keywords:

Abstract

This paper represents the uniform distribution of particles in a mixture of Silicon Nitride and Hexagonal Boron Nitride using Ball milling process. Here, a novel attempt is made to quantify the uniform distribution of particles in terms of the Experimental Fraction of Observations. The effects of process parameters on Average Particle Size and Experimental Fraction of Observations were studied. Taguchi Methodology was used for Design of Experiments in this study. Optimal factor level settings corresponding to the individual responses were found. Analysis of Variance was conducted as well for both the responses. The mean predicted values of responses and the 95% confidence intervals for the same were also calculated. The confirmation test results are found to lie between the predicted confidence Intervals for both the confirmation experiments and population.

Abbreviations

hBN	Hexagonal Boron Nitride	BPR (N)	Ball to Powder Weight Ratio
Si_3N_4	Silicon Nitride	SNRA	Signal to Noise Ratio
APS	Average Particle Size	ANOVA	Analysis of Variance
EFO	Experimental Fraction of Observations	SEM	Scanning Electron Microscopy
DOE	Design of Experiments	DOF	Degrees of Freedom
SSS	Sequential Sum of Squares	MSD	Mean Squared Deviation
AMS	Adjusted Mean Squares	P	Milling Time
O	Milling Speed	hrs	hours

1. Introduction

Ceramics play a vital role in today's era due to their properties like low density, high strength, good chemical inertness and high hardness. These materials have applications in industries, space technology and biomedicine to manufacture cutting tool tips, wear parts, rotors for the turbochargers of diesel engines, dental implants and prostheses (1–3).

Silicon Nitride (Si_3N_4) and Hexagonal Boron Nitride (hBN) are recognized to be the most important engineering ceramics among the ceramic materials. Si_3N_4 has low dielectric constant, high fracture toughness, high strength, low dielectric loss, excellent wear resistance, good oxidation resistance and creep resistance; and Si_3N_4 based ceramics are used to manufacture units and parts operating under severe thermal and mechanical loading (4,5). hBN has properties like low dielectric constant, stable at high temperatures, less chemically reactive, high thermal conductivity, non-toxicity and environmental safety (6,7). Such ceramics find applications in metal industry, chemical engineering, lubricating

*Corresponding author: rarya121212@gmail.com
[a] orcid.org/0000-0002-1809-6333; [b] orcid.org/0000-0001-6120-9746;
DOI: http://dx.doi.org/10.17515/resm2023.800me0614

materials, high temperature furnaces, and thermal protection systems (8). The hBN particles provide a self-lubrication property (9).

Both these ceramics, Si_3N_4 and hBN, were milled together to attain uniform distribution of particles. Ball mill remains the most economical method for this purpose and was used to homogenize the distribution of particles and making finer mixture (10). There are several process variables affecting the outcome of the ball milling process. Pengfei Zhang et al. (11) researched the structure of SiBCN powders while performing ball milling. They studied the impact of speed, Ball to Powder Weight Ratio (BPR) and milling time on the morphology of powder. Pardeep Sharma et al.(12) had mechanically alloyed B_4C (more than 99.6% purity) and Si_3N_4 powder for 100 hrs of milling time. Hongju Qiu et al.(13) prepared nano-sized $6MgO–2Y_2O_3–ZrO_2$ powders by combining ball mill and co-precipitation. They studied the impact of milling time on ZrO_2 crystal particles. N. Hlabangana et al. (14) varied the grinding media size and feed material particle size distribution to optimize the milling efficiency. Grinding media filling, powder filling and the mill rotational speed were constant parameters in their study. A. Wagih et al. (15) had used a dynamic model to anticipate the particle size after the ball mill. Ball size, milling time and milling speed were the parameters optimized by them. S. Tahamtan et al. (16) used ball milling to mill Alumina powder with Al and Mg so as to use this mixture for further stir casting process. Fatih Erdemir (17) investigated the impact of ball milling input parameters on the particle size and X-ray peak ratios using RSM.

From literature survey, it is revealed that there has been almost a complete dearth of literature on optimization of process parameters of Ball Milling process using Design of Experiments (DOE) approach. A novel term Experimental Fraction of Observations (EFO) has been proposed by the authors in the literature to quantify the uniform distribution of particles. In this research study, a novel attempt has been made to ascertain the optimal settings of the ball milling process parameters for achieving optimal values Average Particle Size (APS) and EFO using Taguchi's Design of Experiments approach.

2. Experimental Details:

The procedure from raw material selection to the confirmation tests is shown in Fig. 1.

2.1. Machine Used

The jar milling machine available at Advance Tribology Lab of the Institute was used to homogenize the powders. The diameter of the balls used was 6mm in the ball milling process.

2.2. Raw Materials

The Si_3N_4 and hBN were used as the raw materials with purity level of 99.5%. The APS range of both powders was 5-50 microns as procured from the supplier. The Scanning Electron Microscopy (SEM) images of raw Si_3N_4 and hBN are shown in Fig. 2 (a) and Fig. 2 (b) respectively.

2.3. Selection of Process Parameters

Milling Time, BPR, and Milling Speed were the three process variables chosen for ball milling process. These were selected based on literature survey and pilot experimentation using One Variable at a Time Approach. The ranges of these parameters are given in Table 1.

2.4. Measurement of responses

APS and EFO were the responses considered in this research work. The APS was calculated by taking the average of 320 observations of particle size from SEM images. There were a total of four SEM images taken from four different locations from the same sample. The scale for SEM image was fixed to 50 μm. Then 80 readings of particle size were taken from each SEM image.

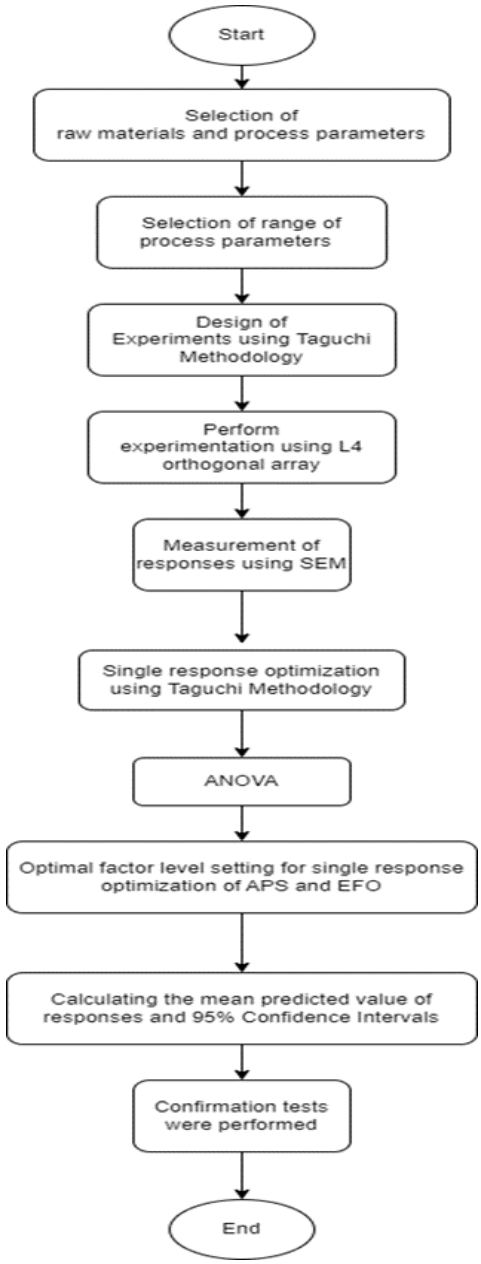

Fig. 1 Experimental methodology

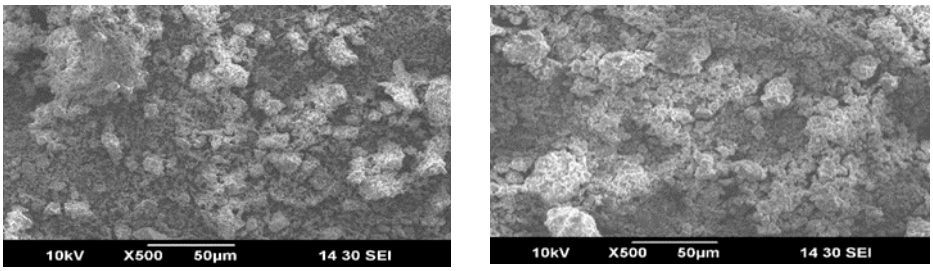

(a) (b)

Fig. 2 (a) SEM image of Silicon Nitride; 2(b) SEM image of Hexagonal Boron Nitride

Table 1. Range of process parameters

Process Parameters	Range
Milling Time	1.5-2.5 hrs
BPR	8:1-12:1
Milling Speed	300-500 rpm

ImageJ software was used to calculate APS. A novel parameter EFO was proposed in this study to quantify the uniform distribution of particles which is given by Equation 1. The uniform distribution of particles was quantized in terms of observations falling under 4 sigma (σ) limit. This level of performance yields a product that is free from defects 99.349% of the time.

$$Exp.\,fraction\ of\ observations\ (EFO) = \frac{Number\ of\ observations\ \ within\ 4\sigma\ limits}{Total\ number\ of\ observations} \quad (1)$$

Here, the 4 σ limits= mean ± 2 σ; σ = Standard Deviation

So, the number of observations falling between mean ± 2 σ and divided by the total number of observations is the EFO. The EFO is calculated by ImageJ software and Origin software. The Origin software was used to plot the Histogram according to APS. The calculations for EFO are reported in Table 2 corresponding to 1st set of replicated experiments.

2.5. Experimental Design Methodology

DOE is a statistical method which facilitates to plan, gather data, statistically examine and look into the effect of more than one process parameter simultaneously on the response (18). Taguchi methodology is a technique which helps to study, analyze and optimize the influence of different process parameters simultaneously on the responses using Orthogonal Array and Signal to Noise Ratio (SNRA). The SNRA determines the most robust combination of input process parameters from variation within the results. By maximizing the SNRA, the loss associated can be minimized (19).

Table 2. Calculated values of EFO for 1st set of replicated experiments

	Particle size (μm) lower limit (m-2sigma)	Particle size(μm) upper limit (m+2 sigma)	Particles falling under m+4sigma limit	EFO
Experiment 1	3.2879	19.2634	309	0.9656
Experiment 2	3.1174	26.4207	307	0.9594
Experiment 3	4.8810	19.7800	310	0.9688
Experiment 4	4.3680	17.5171	311	0.9719

$$MSD_{SB} = \frac{1}{N}\sum_{k=1}^{N} x_k^2 \quad (2)$$

$$MSD_{LB} = \frac{1}{N}\sum_{k=1}^{N} \frac{1}{x_k^2} \quad (3)$$

Where N=No. of repetitions, x_k=value of characteristic in k^{th} observation

$$SNRA = -10 \log MSD \quad (4)$$

Table 3. Experimental data for APS

S.No.	Milling Time (hrs)	BPR	Milling Speed (rpm)	APS (μm)			
				R1	R2	R3	SNRA value
1	1.5	8:1	300	11.2757	10.9642	11.1052	-20.9188
2	1.5	12:1	500	14.7909	14.5981	14.6751	-23.3394
3	2.5	8:1	500	12.3305	12.5725	12.8832	-22.0057
4	2.5	12:1	300	10.9425	10.5698	10.7258	-20.6259

Table 4. Experimental data for EFO

S.NO.	Milling Time (hrs)	BPR	Milling Speed (rpm)	EFO			
				R1	R2	R3	SNRA value
1	1.5	8:1	300	0.9656	0.9658	0.9655	-0.3038
2	1.5	12:1	500	0.9594	0.9599	0.9591	-0.3594
3	2.5	8:1	500	0.9688	0.9690	0.9685	-0.2756
4	2.5	12:1	300	0.9719	0.9699	0.9709	-0.2565

In this paper, Taguchi methodology was used for DOE. L4 orthogonal array was selected as an experimental design matrix for investigating three factors having two levels each. The nature of APS was minimizing in nature, so Mean Squared Deviation (MSD) formula for 'Smaller the Better' type of response was used to calculate SNRA as given by Equations 2 and 4. The MSD for 'Larger the better' type of response was considered to calculate SNRA

for EFO as this response was maximizing in nature given by Equations 3 and 4. Tables 3 and 4 represent the calculated values of APS and EFO corresponding to Taguchi's L4 array with 3 replications. The SNRA values have also been included in the last columns of the Tables.

3. Results and Discussions

The average particle sizes of raw Si_3N_4 and hBN were calculated as 14.5997 µm and 20.9046 µm respectively as shown in Fig. 3 (a) and Fig. 3 (b). The Fig. 2(a) and Fig. 2(b) depict non- uniform distribution of particles of Si_3N_4 and hBN. The range of particle size for hBN was from 4.5100 µm to 90.8430 µm and it was from 3.9520 µm to 49.8010 µm for Si_3N_4. The standard deviations for Si_3N_4 and hBN were calculated as 8.1089 µm and 14.3121µm respectively. After performing ball milling process according to DOE, a uniform distribution of particle size was revealed as shown in Fig. s 4 (a-d) and Fig. 5 (a-d). The Fig. 4 (a) and Fig. 5 (a) correspond to experiment no. 1 with experimental setting of 1.5 hrs of Milling Time, BPR of 8:1 and Milling speed of 300 rpm. Similarly, Fig. 4 (b) & Fig. 5 (b), Fig. 4 (c) & 5 (c), and Fig. 4 (d) & 5 (d) correspond to experiment numbers 2, 3, and 4 respectively. The particle size and standard deviations improved which resulted in the reduction of the spread of the normal distribution curve corresponding to 4 different experimental settings. The 1st replication for experiments resulted in the standard deviation of 3.9939 µm, 5.8367 µm, 3.7248 µm and 3.2873 µm respectively. The APS was improved and lies between 10.5698 µm and14.7910 µm for all 4 experiments.

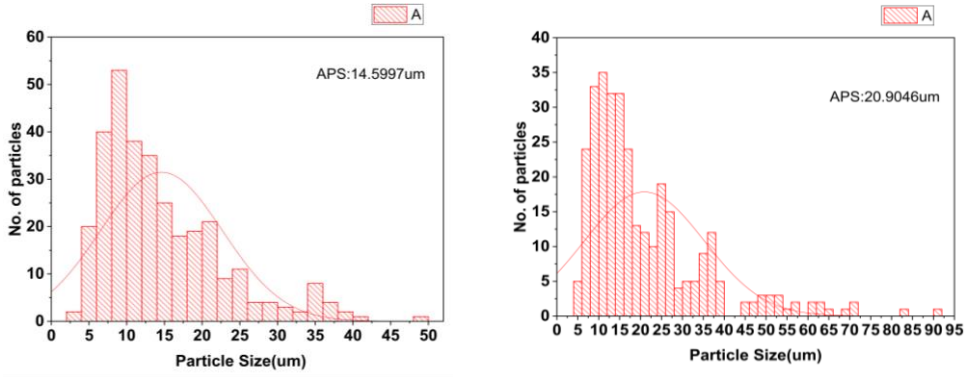

(a) (b)

Fig. 3 (a, b): Particle size distribution for hBN and Si_3N_4

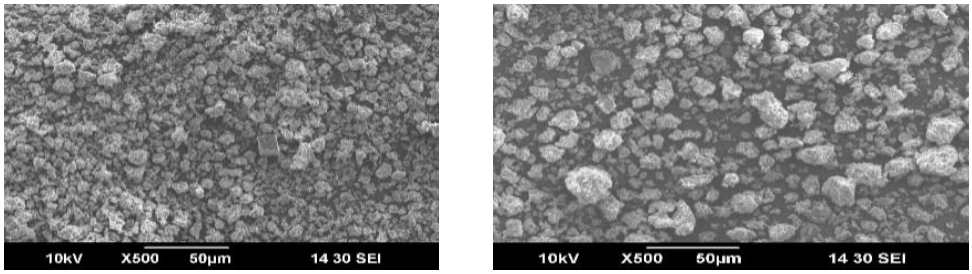

(a) corresponding to experiment no.1 (b) corresponding to experiment no.2

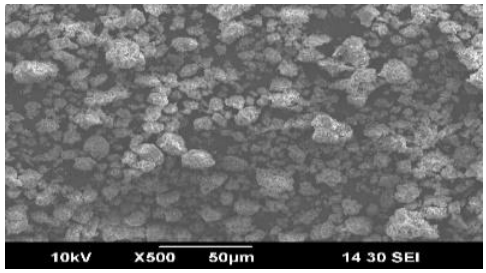

(c) corresponding to experiment no.3

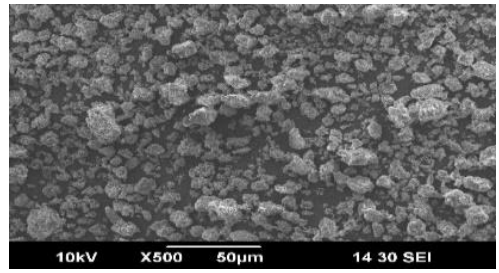

(d) corresponding to experiment no.4

Fig. 4 (a-d): SEM images corresponding to Experimental Design

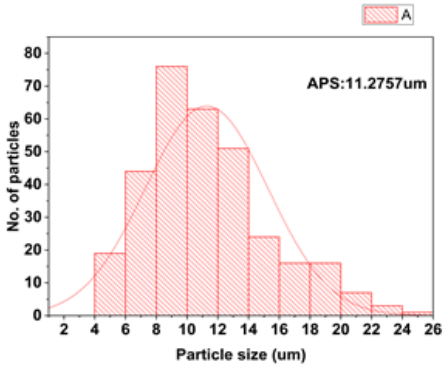

(a) corresponding to experiment 1

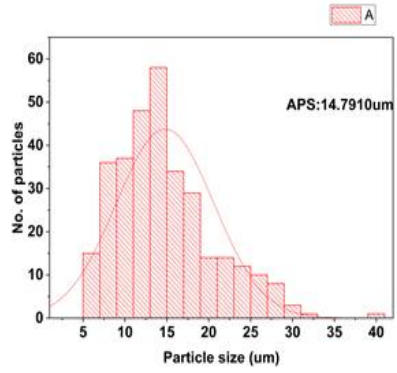

(b) corresponding to experiment 2

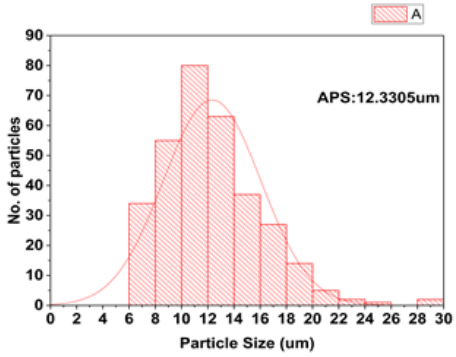

(c) corresponding to experiment 3

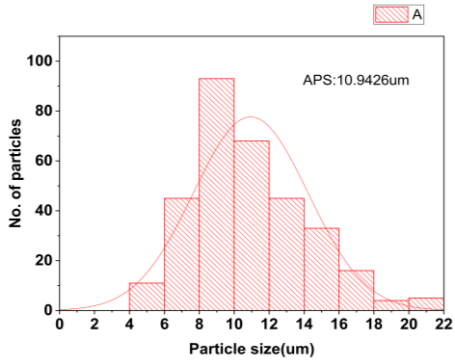

(d) corresponding to experiment 4

Fig. 5 (a-d): Histogram plots corresponding to experimental design

3.1 Influence of input factors on APS and EFO

The APS decreased as the milling time increased from 1.5 hrs to 2.5 hrs. The APS increased with increase in BPR from 8:1 to 12:1 and it also increased with increase in milling speed from 300 rpm to 500 rpm as shown in Fig. 6. The ball milling process resulted in increased EFO as the milling time changes from 1.5 hrs to 2.5 hrs. The EFO decreased with increase in BPR and milling speed as shown in Fig. 7.

Fig. 6 Main effects plot for means and SNRA for APS

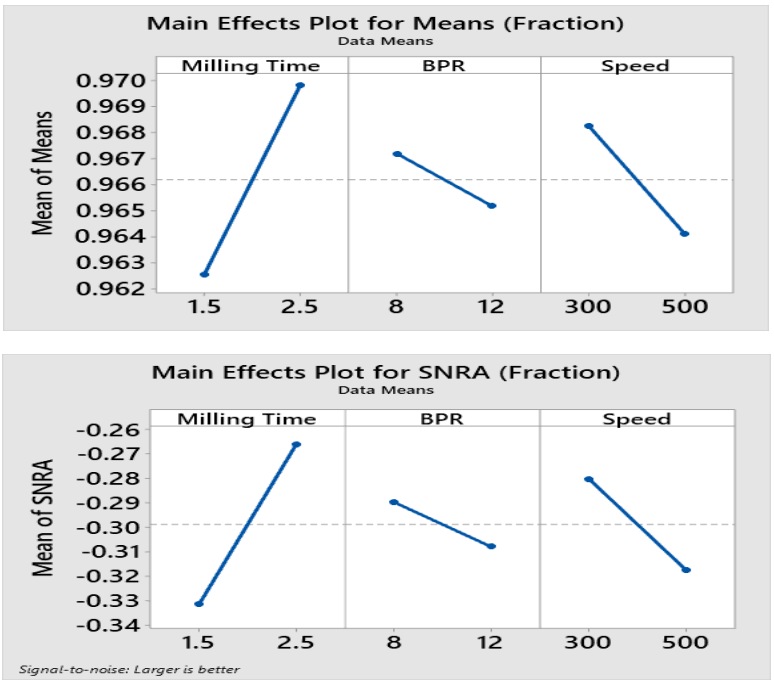

Fig. 7 Main effects plot for means and SNRA for EFO

3.2 Analysis of Responses

Analysis of Variance (ANOVA) is a statistical tool to determine the percentage contribution and significance of different factors on the selected response. The F-ratio test is a very widely used and trusted test for ascertaining the significance of the factors in any study. A factor is said to be significant at some stated level of confidence, say 95%, if the calculated value of F-ratio statistic for that factor is greater than the tabulated value of F-ratio for that factor (20).

Here, the tabulated value of F-ratio is 5.32 and all the calculated values are much greater than the tabulated F-value; hence all the factors are statistically significant in affecting the APS at 95% confidence level as given in Table 5. The most contributing factor was Milling Speed with 75.74% contribution, followed by Milling Time and BPR in that order.

Table 5. ANOVA table for average particle size

Source	DOF	SSS	Contribution	AMS	F-Value	P-Value
Regression	3	28.8247	99.00%	9.6082	264.05	0.000
Milling Time	1	4.5447	15.61%	4.5447	124.89	0.000
BPR	1	2.2283	7.65%	2.2283	61.24	0.000
Milling Speed	1	22.0517	75.74%	22.0517	606.01	0.000
Error	8	0.2911	1.00%	0.0364		
Total	11	29.1158	100.00%			
Tabulated F-value: $F_{0.05}(1,8) = 5.32$						

Similarly, for EFO, the calculated F-Ratios of all the factors are greater than the tabulated F-Ratio as reported in Table 6. Therefore, all the factors are statistically significant at 95% confidence level in affecting EFO. The most contributing factor was Milling Time with 70.57% contribution, followed by Milling Speed and BPR in that order.

Table 6. ANOVA table for EFO

Source	DOF	SSS	Contribution	AMS	F-Value	P-Value
Regression	3	0.000223	98.89%	0.000074	237.88	0.000
Milling Time	1	0.000159	70.57%	0.000159	509.25	0.000
BPR	1	0.000012	5.41%	0.000012	39.04	0.000
Milling Speed	1	0.000052	22.91%	0.000052	165.34	0.000
Error	8	0.000002	1.11%	0.000000		
Total	11	0.000226	100.00%			
Tabulated F-value: $F_{0.05}(1,8) = 5.32$						

3.3 Optimization and Predicted Value

The average particle size of the powder is a smaller the type of quality characteristic and the lowest points in the main effects plot for the means will correspond to the optimal settings of the process parameters leading to the best response. The EFO, on the other hand, is a larger the better type of quality characteristic and the highest points in the main effects plot for the means will correspond to the optimal settings of the process parameters resulting in the optimal value of the response.

As regards SNRA plots, the highest points in the plot will always correspond to the optimal settings of the factors leading to the best value of the response irrespective of the fact whether the quality characteristic is either smaller the better or larger the better.

Accordingly, Fig. 6 and Fig. 7 have been analysed for obtaining optimal settings of the parameters for individual responses. Second level of milling time, first level of BPR and first level of milling speed correspond to the highest points in SNRA ratio plots for APS as well as EFO. Hence, these values represent the optimal settings of the selected parameters for obtaining the best responses.

The predicted optimal value of APS corresponding to the optimal values of process parameters has been obtained by using Equation 5. Similar procedure was then adopted to find the predicted optimal value of EFO.

$$M_{APS} = \overline{P_2} + \overline{N_1} + \overline{O_1} - 2\overline{T} \quad (5)$$

Where $\overline{T}$ is the overall mean of APS=$(\sum R_1 + \sum R_2 + \sum R_3)/12$

$\overline{P_2}$= Mean value of APS at level 2 of Milling Time

$\overline{N_1}$= Mean value of APS at level 1 of BPR

$\overline{O_1}$= Mean value of APS at level 1 of Milling Speed

The predicted optimal values for both the quality characteristics are given in Table 7. The SEM image of powder after performing ball mill at optimal factor setting is depicted in Fig. 8.

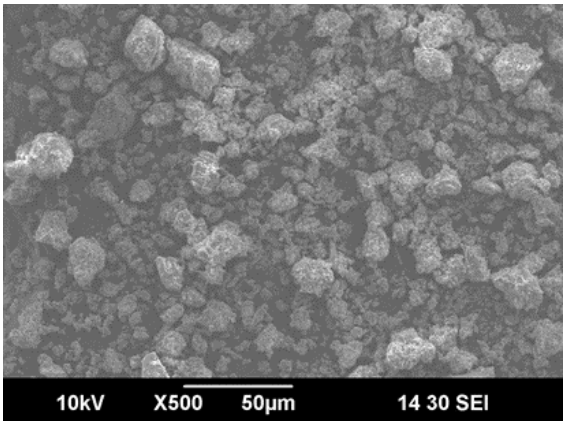

Fig. 8 SEM image of confirmation experiment

The 95% Confidence Intervals corresponding to Population and Confirmation Experiments were calculated by the using Equations 6 & 7.

$$CI_{CE} = \sqrt{(F_\alpha\ (1, d_e)E_v\left(\frac{1}{n_{eff}} + \frac{1}{A}\right)} \quad (6)$$

$$CI_{POP} = \sqrt{\frac{(F_\alpha\ (1, d_e)E_v}{n_{eff}}} \quad (7)$$

where, $F_\alpha\ (1, d_e)$= The F ratio at the confidence level of (1-α) against DOF of mean, which is equal to 1, and error degrees of freedom d_e.

$$n_{eff} = \frac{N}{1+[\text{DOF associated in the estimateof mean response}]} = 12 / (1+3) = 3$$

N = Total number of Observations = 4 x 3 = 12; A = Sample size for confirmation experiments = 3

E_v = Error variance (from ANOVA Table); d_e = error DOF = 8; $F_{0.05}\ (1, 8) = 5.32$

Table 7. Optimal factor level setting

1.	APS	2.5(P_2)	8:1(N_1)	300(O_1)	9.8842 µm
2.	EFO	2.5(P_2)	8:1(N_1)	300(O_1)	0.9729

The predicted values of confidence intervals at 95% confidence level for both the responses are reported in Table 8. The confirmation tests were performed at the optimal factor level setting and the average values of the confirmation experiments are found to lie within the predicted 95% confidence intervals as given in Table 8.

Table 8: Predicted values of confidence intervals at 95% level

Output Process Parameters	Input Optimal Process Parameters Settings	Predicted Confidence Intervals at 95% Confidence Level	Mean of three confirmation experiments
APS	$P_2N_1O_1$	CI_{CE} : 9.5249 < μ_{APS} < 10.2435 CI_{POP} : 9.6301 < μ_{APS} < 10.1382	10.1234 µm
EFO	$P_2N_1O_1$	CI_{CE} : 0.9720 < μ_{EFO} < 0.9738 CI_{POP} : 0.9722 < μ_{EFO} < 0.9736	0.9723

4. Conclusions

In this research article, optimization of ball milling process parameters for APS and EFO was accomplished through Taguchi's DOE approach. Here, Orthogonal array L4 was selected and experiments were replicated 3 times. The number of observations falling under 4 σ limit was utilized to quantize the uniform distribution of particles. EFO term was coined for uniform distribution of particles. The nature of APS was minimizing and that of EFO was maximizing. Therefore, the SNRA for APS was chosen as per lower the better type of response, whereas the SNRA for EFO was chosen as per larger the better type of quality characteristic. The following conclusions were drawn from this paper:

- The ball milling process resulted in decreasing the range of Average Particle Size from 14.59972 µm-20.90461 µm to 10.5698-14.7909 µm.
- The standard deviation range of Average Particle Size improved from 8.10889µm-14.3121 µm to 3.2873 µm - 5.8367 µm, i.e., most of the particles were of the same size.
- Experimental Fraction of Observations for the 4sigma limit resulted in uniform distribution of the particles.
- Milling speed, milling time and Ball to powder weight ratio were found as significant factors at 95% confidence level for both Average Particle Size and Experimental Fraction of Observations.
- The most significant factor affecting the Average Particle Size was the Milling Speed with 75.74% contribution.

- The most significant factor for Experimental Fraction of Observations was the milling time with 70.57% contribution.
- Milling Time of 2.5 hrs, Ball to Powder Weight Ratio of 8:1 and Milling Speed of 300rpm were optimal factor level settings for both Average Particle Size and Experimental Fraction of Observations.
- The confirmation tests were performed and the average values of responses were found to lie between the predicted 95% confidence intervals for both confirmation experiments and population.
- Authors have coined and introduced a novel quality characteristic, Experimental Fraction of Observations, to represent a measure of uniform distribution of particles in ball milling process.

Declarations

Conflict of Interest: The authors do not have any conflicts of interest.

Data Availability Statement

All data that support the findings of this study are included within the article (and any supplementary files).

Author Contribution:
Rashmi Arya: Conceptualization, Methodology, Investigation, Writing - original draft, analysis. Hari Singh: Conceptualization, Supervision. Writing - review & editing, Methodology.

References

[1] Lok YK, Lee TC. Processing of advanced ceramics using the wire-cut EDM process. Journal of Materials Processing Technology. 1997;63(1-3):839-43. https://doi.org/10.1016/S0924-0136(96)02735-5
[2] Zhang C. Study of small cracks on nanocomposite ceramics cut by WEDM. International Journal of Advanced Manufacturing Technology. 2016;83(1-4):187-92. https://doi.org/10.1007/s00170-015-7569-1
[3] Ming W, Jia H, Zhang H, Zhang Z, Liu K, Du J, et al. A comprehensive review of electric discharge machining of advanced ceramics. Ceramics International [Internet]. 2020;46(14):21813-38. https://doi.org/10.1016/j.ceramint.2020.05.207
[4] Zakorzhevsky V V. Silicon Nitride. In: Concise Encyclopedia of Self-Propagating High-Temperature Synthesis [Internet]. Elsevier Inc.; 2017. p. 339-41. https://doi.org/10.1016/B978-0-12-804173-4.00134-4
[5] Liang G, Sun G, Bi J, Wang W, Yang X, Li Y. Mechanical and dielectric properties of functionalized boron nitride nanosheets/silicon nitride composites. Ceramics International [Internet]. 2021;47(2):2058-67. https://doi.org/10.1016/j.ceramint.2020.09.038
[6] Wang J, Ma F, Sun M. Graphene, hexagonal boron nitride, and their heterostructures: properties and applications. RSC Advances. 2017;7(27):16801-22. https://doi.org/10.1039/C7RA00260B
[7] Eichler J, Lesniak C. Boron nitride (BN) and BN composites for high-temperature applications. Journal of the European Ceramic Society. 2008;28(5):1105-9. https://doi.org/10.1016/j.jeurceramsoc.2007.09.005
[8] Duan X, Yang Z, Chen L, Tian Z, Cai D, Wang Y, et al. Review on the properties of hexagonal boron nitride matrix composite ceramics. Journal of the European Ceramic Society. 2016;36(15):3725-37. https://doi.org/10.1016/j.jeurceramsoc.2016.05.007
[9] Gnanavelbabu A, Rajkumar K. Experimental Characterization of Dimensional and Surface Alternation of Straight and Angular Cutting on Self-lubricating Composite: A

Wire EDM Approach. Arabian Journal for Science and Engineering [Internet]. 2020;45(7):5859-72. https://doi.org/10.1007/s13369-020-04596-2

[10] Ahmadian H, Sallakhniknezhad R, Zhou T, Kiahosseini SR. Mechanical properties of Al-Mg/MWCNT nanocomposite powder produced under different parameters of ball milling process. Diamond and Related Materials [Internet]. 2022;121(September 2021):108755. https://doi.org/10.1016/j.diamond.2021.108755

[11] Zhang P, Jia D, Yang Z, Duan X, Zhou Y. Influence of ball milling parameters on the structure of the mechanically alloyed SiBCN powder. Ceramics International [Internet]. 2013;39(2):1963-9. https://doi.org/10.1016/j.ceramint.2012.08.047

[12 Sharma P, Khanduja D, Sharma S. Metallurgical and mechanical characterization of Al 6082- B4C/Si3N4 hybrid composite manufactured by combined ball milling and stircasting. Applied Mechanics and Materials. 2014;592-594:484-8. https://doi.org/10.4028/www.scientific.net/AMM.592-594.484

[13] Qiu H, Huang W, Zhang Y, Chen J, Gao L, Omran M, et al. Preparation of nano-sized 6MgO-2Y2O3-ZrO2 powders by a combined co-precipitation and high energy ball milling process. Ceramics International [Internet]. 2022;48(13):19166-73.

[14] Hlabangana N, Danha G, Muzenda E. Effect of ball and feed particle size distribution on the milling efficiency of a ball mill: An attainable region approach. South African Journal of Chemical Engineering [Internet]. 2018;25:79-84. https://doi.org/10.1016/j.sajce.2018.02.001

[15] Wagih A, Fathy A, Kabeel AM. Optimum milling parameters for production of highly uniform metal-matrix nanocomposites with improved mechanical properties. Advanced Powder Technology [Internet]. 2018;29(10):2527-37. https://doi.org/10.1016/j.apt.2018.07.004

[16 Tahamtan S, Halvaee A, Emamy M, Zabihi MS. Fabrication of Al/A206-Al2O3 nano/micro composite by combining ball milling and stir casting technology. Materials and Design [Internet]. 2013;49:347-59. https://doi.org/10.1016/j.matdes.2013.01.032

[17] Erdemir F. Study on particle size and X-ray peak area ratios in high energy ball milling and optimization of the milling parameters using response surface method. Measurement: Journal of the International Measurement Confederation [Internet]. 2017;112(July):53-60. https://doi.org/10.1016/j.measurement.2017.08.021

[18] Arya R, Singh H. Optimization of Wire-cut EDM process parameters using TLBO algorithm. Engineering Research Express. 2022;4(3):035051. https://doi.org/10.1088/2631-8695/ac8fcc

[19] Garg R. Effect Of Process Parameters On Performance Measures Of Wire Electrical Discharge Machining [Internet]. Vol. Ph.D. National Institute Of Technology, Kurukshetra-136 119, Haryana, India; 2010. Available from: http://nitkkr.ac.in/nit_kuk/docs/Ph.D._Thesis_by_Rohit_Garg.pdf

[20] Ross PJ. Taguchi Techniques for Quality Engineering. 2nd ed. McGraw-Hill Education (India) Pvt Limited; 2005.